Volume 18 • Issue 4 • June 2015

ECOSYSTEMS

Cover Photo of Oregon Forest After Wildfire

Under-ice and Hypolimnion Contribution to CO_2 Emission from Lakes

Growth Decline Affects Beech But Not Other Broad-leaved Trees in Central Europe

Biogeochemical Effects of Nesting Cormorants

Large Herbivores and Terrestrial Subsidies to Stream Food Webs

Springer

10021 • ISSN 1432 9840
18:4 547–734 (2015)

Ecosystems (2015) 18: 573–588
DOI: 10.1007/s10021-015-9847-z

ECOSYSTEMS

Disturbance and Topography Shape Nitrogen Availability and δ^{15}N over Long-Term Forest Succession

Steven S. Perakis,[1]* Alan J. Tepley,[2] and Jana E. Compton[3]

[1]*U.S. Geological Survey, Forest and Rangeland Ecosystem Science Center, Corvallis, Oregon 97331, USA;* [2]*Department of Geography, University of Colorado, Boulder, Colorado 80309, USA;* [3]*National Health and Environmental Effects Research Laboratory, Western Ecology Division, U.S. Environmental Protection Agency, Corvallis, Oregon 97333, USA*

ABSTRACT

Forest disturbance and long-term succession towards old-growth are thought to increase nitrogen (N) availability and N loss, which should increase soil δ^{15}N values. We examined soil and foliar patterns in N and δ^{15}N, and soil N mineralization, across 800 years of forest succession in a topographically complex montane landscape influenced by human logging and wildfire. In contrast to expectations, we found that disturbance caused declines in surface mineral soil δ^{15}N values, both in logged forests measured 40–50 years after disturbance, and in unlogged forests disturbed by severe wildfire within the last 200 years. Both symbiotic N fixation and N transfers from disturbed vegetation and detritus could lower soil δ^{15}N values after disturbance. A more important role for symbiotic N fixation is suggested by lower soil δ^{15}N values in slow-successional sites with slow canopy closure, which favors early-successional N fixers. Soil δ^{15}N values increased only marginally throughout 800 years of succession, reflecting soil N uptake by vegetation and strong overall N retention. Although post-disturbance N inputs lowered surface soil δ^{15}N values, steady-state mass balance calculations suggest that wildfire combustion of vegetation and detritus can dominate long-term N loss and increase whole-ecosystem δ^{15}N. On steeper topography, declining soil δ^{15}N values highlight erosion and accelerated soil turnover as an additional abiotic control on N balances. We conclude for N-limited montane forests that soil δ^{15}N and N availability are less influenced by nitrate leaching and denitrification loss than by interactions between disturbance, N fixation, and erosion.

Key words: fire; logging; erosion; nitrogen isotope; nitrogen mineralization; nitrogen fixation.

INTRODUCTION

Natural abundance isotopes of nitrogen (N) can be an effective tool for integrating ecosystem N cycling and N input–output balances. Nitrogen isotopes in soil can be particularly effective integrators because soil is generally the largest N pool in most terrestrial ecosystems. Both N input and loss pathways are important in shaping N balances, yet not all of these fluxes are easily quantified with field measurement. In these cases, N isotopes can be used to infer fluxes where field measurements are lacking (Bai and others 2012). Such quantitative use of natural abundance N isotopes to infer long-term ecosystem N fluxes often assumes steady-state

---

Received 6 May 2014; accepted 6 January 2015;

Electronic supplementary material: The online version of this article (doi:10.1007/s10021-015-9847-z) contains supplementary material, which is available to authorized users.
Author contributions SSP and JEC conceived the study and performed research. SSP and AJT analyzed data. SSP wrote the paper with input from JEC and AJT.
**Corresponding author; e-mail:* steven.perakis@oregonstate.edu

conditions. Although this may be applicable in some regions, steady-state conditions may be less common in disturbance-prone ecosystems that display slow trajectories of recovery following large-scale disturbance (Vitousek and Reiners 1975; Weisberg and Swanson 2003). Steady-state conditions may also be less common in the future as human activities increasingly modify both disturbance regimes and N cycling worldwide (Vitousek and others 1997). Understanding how disturbance shapes ecosystem N fluxes, particularly over long time scales, would improve the use of N isotopes for inferring controls on ecosystem N balances, and for predicting how ecosystems will respond to altered disturbance regimes in the context of on-going climatic and land-use change.

Disturbances can influence ecosystem N budgets and cycling via several pathways that cause transient increases in soil δ^{15}N values. Direct effects of disturbance include the removal of biomass and detritus with characteristically low δ^{15}N values, leaving behind mineral soil of relatively high soil δ^{15}N values as N cycling recovers (Högberg 1997). Disturbance also disrupts plant N uptake, which can increase fractionating N loss via nitrate leaching and denitrification, leading to higher soil δ^{15}N values (Pardo and others 2002). Disturbance-driven increases in soil δ^{15}N values should be greatest in ecosystems with high-N availability and potential for fractionating N loss. In contrast, soil δ^{15}N values of low-N ecosystems may be relatively complacent to disturbance due to low fractionating N loss, and instead may reflect post-disturbance N inputs.

Wildfire is the primary natural disturbance agent in many forest ecosystems worldwide (Bowman and others 2009), and can strongly affect ecosystem N cycling and δ^{15}N values (Grogan and others 2000; Smithwick and others 2005; Hyodo and others 2013). Combustion of plants and detritus removes ^{15}N-depleted gases, leading to higher δ^{15}N values in residual ash and char (Turekian and others 1998; Saito and others 2007; Huber and others 2013). Organic matter combustion also liberates available N that can increase leaching and gaseous N loss (Johnson and others 2004). Together, these losses should increase soil δ^{15}N values, yet field studies show both increases and decreases in soil δ^{15}N after fire, suggesting post-disturbance processes also shape soil δ^{15}N values (Aranibar and others 2003). A better understanding of how fire shapes soil δ^{15}N values over succession and larger landscapes is needed to clarify both the short-term effects of fire on N cycling, and for interpreting long-term studies and paleo-records that link disturbance and biogeochemistry (McLauchlan and others 2014; Dunnette and others 2014). Spatially extensive landscape-scale sampling of surface mineral soil δ^{15}N values may be particularly informative, as surface soils display the strongest δ^{15}N response to logging and wildfire (Pardo and others 2002; Boeckx and others 2005).

Patterns of vegetation establishment, regrowth, succession, and associated changes in N cycling can be important in shaping soil δ^{15}N values after disturbance. Post-disturbance plant growth redistributes N with low δ^{15}N values from soil to aboveground biomass, which increases soil δ^{15}N values over time (Compton and others 2007). This N redistribution can be species-specific (McLauchlan and Craine 2012) and vary with site productivity (Kranabetter and others 2013) or N availability (Perakis and others 2011). The pattern and pace of vegetation succession may also affect N redistribution, N inputs, and soil δ^{15}N values, but data to evaluate this idea are scarce. For example, individual emergent canopy trees that scavenge N from aerosols may leave local imprints on soil N availability and δ^{15}N values relative to surrounding vegetation (Perakis and Kellogg 2007). In addition, early-successional vegetation often includes symbiotic N-fixing species, especially in fire-prone regions (Rastetter and others 2001; Menge and others 2010). Nitrogen fixation typically adds N near the isotopic value of atmospheric N_2 ($\delta^{15}N = 0‰$), which may shift soil δ^{15}N values closer to that of fixed N (Shearer and Kohl 1989; Stock and others 1995; Grogan and others 2000; Barrett and others 2002; Aranibar and others 2003; Boutton and Liao 2010; Bai and others 2013). Such N fixation legacies on soil δ^{15}N may even persist after fixers are replaced by non-N-fixing vegetation, due to the relatively long residence time of N in soil (Scott and others 2008; Perakis and others 2011). Indeed, symbiotic N fixation often dominates ecosystem N inputs in early-succession after fire (Yelenik and others 2013), suggesting that soil δ^{15}N values may yield new insights into how symbiotic N fixation shapes long-term N balances in disturbance-prone forests.

We examined soil and foliar N and δ^{15}N patterns, and soil N mineralization, across 60 study plots in and around the HJ Andrews Experimental Forest in the central Oregon Cascade Mountains. Wildfire is the dominant natural forest disturbance in this region, with additional disturbance from clear-cut logging throughout the twentieth century. We took advantage of fire-history studies that document wildfire severity from the late twelfth to the early twentieth century, as well as paired experimental watersheds and plots subject to logging and broadcast burning since the mid-twentieth century, to evaluate how disturbance, climate, topography, and soil N availability shape forest $\delta^{15}N$ values across the landscape. We also consider how symbiotic N fixation by early-successional vegetation may affect N biogeochemistry and soil $\delta^{15}N$ values after disturbance. Specifically, we sought to address the following questions: (1) Do disturbances such as logging and broadcast burning, and natural wildfire, leave legacies of increased soil $\delta^{15}N$ values consistent with higher rates of fractionating N loss, or lower soil $\delta^{15}N$ values consistent with greater post-disturbance N fixation? (2) Does the rate of post-disturbance succession influence soil $\delta^{15}N$ values, and do these changes reflect rates of plant N uptake (that is, increased soil $\delta^{15}N$), biological N fixation (that is, decreased soil $\delta^{15}N$), or soil N availability (that is, span in $\delta^{15}N$ values between plants and soils)? (3) What are the relative roles of ultimate abiotic factors (for example, topography, climate, disturbance) and proximate biotic factors (fractionating N loss, N fixation) in shaping soil $\delta^{15}N$ values over 800+ years of succession in a temperate montane forest landscape? To evaluate N cycling effects on these $\delta^{15}N$ patterns, we also consider how net N mineralization varies in response to biotic and abiotic landscape attributes.

METHODS

Study Sites

We conducted this research in the central Oregon Cascade Mountains, an area of maritime Mediterranean climate with cool wet winters and warm dry summers. Mean monthly temperatures range from 1°C in January to 18°C in July (Bierlmaier and McKee 1989). Soils are primarily Andisols and Inceptisols derived from andesitic and basaltic tuffs and breccias. Forests at lower elevations are dominated by Douglas-fir (*Pseudotsuga menziesii* (Mirb.) Franco), western hemlock (*Tsuga heterophylla* (Raf.) Sarg.), and western red cedar (*Thuja plicata* Donn ex D. Don), and at higher elevations by noble fir (*Abies procera* Rehder), Pacific Silver fir (*A. amabilis* Douglas ex J. Forbes), Douglas-fir, and western hemlock. The sampled stands encompass mesic to relatively dry-site plant associations.

We examined three sets of study sites encompassing 60 plots within and adjacent to the HJ Andrews Experimental Forest (Figure 1). The three sets of study sites include (1) stands of differing successional rate after logging and burning paired with adjacent old-growth forests ($n = 24$ stands total, from Nesje 1996); (2) permanent plots in six gaged watersheds, with three supporting early-successional vegetation and three supporting old-growth forest ($n = 6$ stands total) (Vanderbilt and others 2003), plus six mid-successional plots in the nearby Hagan Block Research Natural Area ($n = 6$ stands, Klopsch 1985); and (3) 24 forest stands from a prior comparison of soil nitrogen and carbon after stand-replacing wildfire (Giesen and others 2008). We collected foliage and soil samples from the first two sets of study sites in summer 2003. The third set of study sites were sampled in summer 2004. More detail on the sites is given below.

The first set of study sites (referred to here as ''Successional Rate'' sites) includes twelve pairs of post-harvest, early-successional stands and adjacent old-growth forest stands ($n = 24$ stands total) in the HJ Andrews Experimental Forest. In the Andrews Forest, harvesting of small patches averaging approximately 10 ha in size was initiated in the 1950s and continued through the 1980s. Using aerial photos, Nesje (1996) classified harvested stands into four stages of development (semi-open, closed mixed shrub, closed mixed trees, and young conifer). These stages were compared using a series of aerial photos on six dates between 1959 and 1990 to identify stands with slow, average, and fast rates of early succession. We omitted Nesje's (1996) ''fast'' category due to confounding effects of stand age, and re-classified the original ''slow'' and ''average'' rates as ''slow'' and ''fast'' for simplicity. This classification into ''slow'' and ''fast'' successional rates is supported by both 1999 field measurements that found significantly greater total plant biomass in fast stands (120 Mg C ha^{-1}) than in slow stands (53 Mg C ha^{-1}, K.E.B. O'Connell and M.E. Harmon, personal communication), and by remotely sensed, ground validated analysis of post-harvest forest recovery rates across 185 km^2 of western Oregon that encompasses our study area (Schroeder and others 2007). These successional rates also fall within the range of estimates for the time to canopy closure following wildfires from the late twelfth to early twentieth century (Tepley and others 2014). Tree cover 17 years after disturbance averaged 40% for slow successional forests and 65% for fast successional forests (Schroeder and others 2007), though all stands had reached canopy closure by the time of our sampling. We randomly selected twelve stands from 19 candidates in Nesje (1996), divided equally between ''slow'' and ''fast'' successional rates, and meeting the criteria of stand area greater than 5 ha, young stand age of approximately 40 years with an immediately adjacent unlogged 400–550-year-old-growth stand,

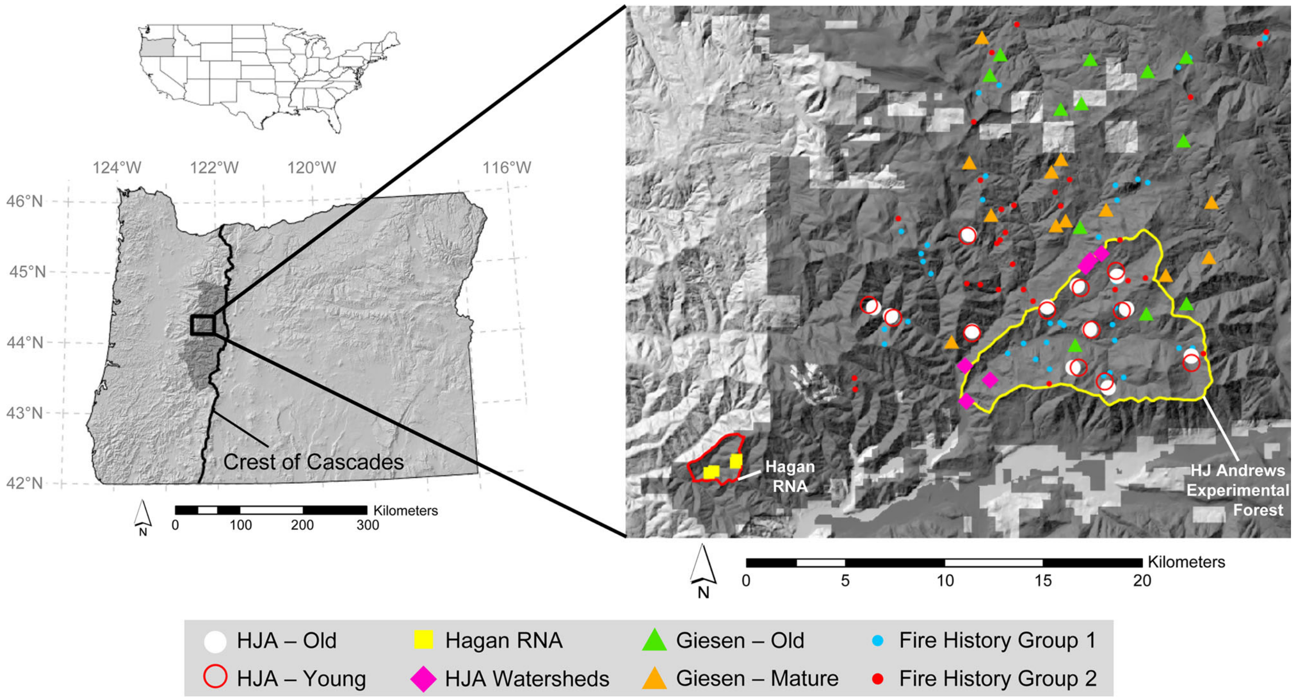

Figure 1. Map of study site locations in and around HJ Andrews Experiment Forest. Dark shading represents the Willamette National Forest (Color figure online).

and topographic/edaphic conditions capable of supporting closed-canopy forests (cliffs and talus slopes were eliminated). This yielded 12 paired young- and old-growth stands (n = 24 stands total). Within a year of logging, all of the young sites were broadcast burned to remove logging slash. Of the slow sites, two were replanted to Douglas-fir, one had natural regeneration, and three have unknown histories. Of the fast sites, three were replanted to Douglas-fir, one had natural regeneration, and two have unknown histories. At the time of sampling, both young and old forests at all sites were dominated by Douglas-fir. There were no significant differences in elevation, slope, aspect, or year of establishment between slow and fast-successional sites (Table 1).

The second set of study sites (referred to here as ‘‘Permanent Plots’’ sites) includes permanent vegetation plots of varying successional stage in and around the HJ Andrews Experimental Forest and in the nearby Hagan Block Research Natural Area (Figure 1). Six sites were located in small watersheds studied as part of the Long Term Ecological Research program (Vanderbilt and others 2003). Three of these watersheds, WS-6, WS-7, and WS-10, support early-successional forests established after logging in 1974–1975. The remaining three old-growth reference watersheds WS-2, WS-8, and WS-10, support approximately 500-year-old forest dominated by Douglas-fir. Due to regional fire history patterns, mid-successional forests (ca. 80–200 years old) are rare at HJ Andrews, but are common in the Hagan Block approximately 11 km to the west (Figure 1). Most stands of the Hagan Block initiated after two overlapping fires around 1855 and 1895 (Klopsch 1985), where we sampled six mid-successional forests approximately 125 years of age.

The third set of study sites (referred to as ‘‘Fire History’’) contains 24 forest stands in the HJ Andrews Experimental Forest and adjacent Willamette National Forest (Figure 1) evaluated in a previous study of long-term soil carbon and nitrogen change after wildfire (Giesen and others 2008). This area experienced a series of wildfires primarily during two periods of region-wide extensive burning across western Washington and Oregon (ca. 1450–1600 and ca. 1800–1940; Weisberg and Swanson 2003). Most stand ages date to one of these periods, and many of the older stands experienced low- or moderate-severity fire in the more recent period of burning (Tepley and others 2013). Twelve old-growth stands were sampled, of which eight initiated in the earlier period of fire (ca. 1450–1600) and four predate these fires with forests over 800 years of age (Giglia 2004). Twelve stands initiated in the more recent period (ca. 1800–1940). For this dataset, we use data on forest floor (that is,

Table 1. Site Characteristics of 60 Forest Stands Examined in This Study

Study stands	*N*	Stand age (years)	Elevation (m)	Slope (%)	MAT (C)	MAP (cm)
Succession rate						
Young-slow	6	43 ± 1.8	912 ± 106	39 ± 7	8.9 ± 0.2	221 ± 4.0
Young-fast	6	47 ± 1.2	880 ± 102	30 ± 7	8.8 ± 0.4	218 ± 5.3
Old-slow	6	~550	925 ± 52	54 ± 7	8.7 ± 0.1	221 ± 4.1
Old-fast	6	~550	914 ± 99	38 ± 8	8.8 ± 0.3	218 ± 5.2
Permanent plots						
WS young	3	29 ± 0.3	836 ± 123	39 ± 18	8.7 ± 0.7	204 ± 8.4
WS old	3	~550	747 ± 153	45 ± 8	9.3 ± 0.8	192 ± 1.3
Hagan block	6	~110	712 ± 21	38 ± 3	10.3 ± 0.1	177 ± 0.9
Fire history						
Mid-successional	12	~150	981 ± 50	35 ± 6	8.2 ± 0.2	220 ± 3.9
Old-growth	12	~550–800+	1113 ± 59	32 ± 3	7.8 ± 0.3	241 ± 6.0

Values are means with standard errors.

O horizon) and 0–10 cm mineral soil C, N, and laboratory net N mineralization reported in Giesen and others (2008), supplemented by stable isotope analyses of forest floor and mineral soil.

Sample Collection and Analysis

The first two sets of study sites described above (that is, Successional Rate and Permanent Plots) were sampled in a single sampling campaign in September 2003. In each plot, we collected eight replicate samples of forest floor, and in the same locations collected mineral soil to 10 cm depth using a 6.9 cm diameter soil corer. Sun-exposed foliage was collected by shotgun from four locations in each plot, and combined into one sample per plot.

Foliage and forest floor were dried at 65°C for 48 h, and mineral soil was sieved (<2 mm) prior to drying at 105°C for 48 h. Subsamples of foliage, forest floor, and mineral soil were ground to a fine powder using a roller mill prior to analysis for total C and N on a Costech ECS-4010 elemental combustion analyzer (Costech Analytical, Valencia, CA, USA) followed by $^{15}N/^{14}N$ on a Finnigan MAT Delta Plus XP mass spectrometer at the Integrated Stable Isotope Research Facility at the Environmental Protection Agency (Corvallis, OR). Isotope values are expressed in standard delta notation (δ) in ‰ units relative to N_2 air standard (Fry 2006). The standard deviation for replicate analyses of $\delta^{15}N$ was less than 0.1‰. We calculated the isotope effect (ϵ_{f-s}) of plant uptake as the difference in $\delta^{15}N$ values between foliage and mineral soil.

Subsamples of sieved fresh mineral soil (0–10 cm) were reserved for additional analyses. Moisture content was determined by drying a 10 g subsample of mineral soil at 105°C for 48 h. Extractable NH_4^+, NO_3^-, total nitrogen, and organic carbon were extracted from 7 g soil for 1 h with 35 mL 0.5 M K_2SO_4, and filtered through Whatman 42 filters. Potential N mineralization was determined by incubating 10 g of fresh soil at 25°C and 60% water holding capacity for 28 days, followed by extraction as above, and corrected for initial NH_4^+ and NO_3^-. Solutions of extractable NH_4^+ and NO_3^- were analyzed colorimetrically using a Lachat RFA 5000A autoanalyzer, and total extractable nitrogen and organic carbon were analyzed by catalytic oxidation combustion using a Shimadzu TOC-V CSH total organic carbon analyzer with a TNM-1 nitrogen unit.

For the third set of study sites (Fire History) we used existing data collected in 2004 on forest floor and mineral soil (0–10 cm) C and N, and laboratory net N mineralization (Giesen and others 2008), and analyzed forest floor and mineral soil $^{15}N/^{14}N$ as described above.

Statistical Analyses

A total of 60 individual forest stands were considered in our analyses, with subsets of stands used for different analyses. In all cases, we calculated the arithmetic mean of replicate subsamples collected within stands, and used this mean value for statistical analyses. In the first analysis of paired young and old plots of differing successional rate ($n = 24$), we used split-plot ANOVA to examine how stand age (young vs. old) and successional rate (slow vs. fast) influenced soil and foliar response variables.

In the second analysis, we analyzed the full dataset ($n = 60$) using Bayesian Information Criterion (BIC) and linear regression to evaluate how stand age, fire disturbance history, climate, topography, and soil characteristics influenced soil δ^{15}N and net N mineralization across sites. We used BIC rather than AIC, because BIC is less prone to overfitting multiple predictor variables in large datasets (Murtaugh 2009). We used 16 predictor variables for which we had data for all sites. Mean annual temperature, mean annual precipitation, and climatic moisture deficit (that is, potential minus actual evapotranspiration, Stephenson 1998) were derived from latitude, longitude, and elevation by ClimateWNA, based on PRISM model interpolation for the period 1971–2000 (Wang and others 2012). Slope and aspect were derived from 10 m digital elevation models, and heat load was estimated from incident solar irradiance (MJ cm^{-2} year) folded on SSW aspect (McCune 2007). In stands that originated after wildfire, we considered stand age as the age of the oldest living tree sampled at the nearest plot in previous fire-history studies (Klopsch 1985; Weisberg and Swanson 2003; Giglia 2004). For logged stands, ages were based on discrete vegetation establishment dates (Nesje 1996). Because of the prevalence of less intense non-stand-replacing wildfire in this region, we also used a metric of more recent fire history adapted from Tepley and others (2013). Finally, we also considered forest floor concentrations of C, N, and carbon-to-nitrogen (C:N) mass ratio, surface mineral soil (0–10 cm) concentrations of C, N, and C:N, potential net N mineralization and percent nitrification. For these 16 predictor variables, we considered models within 3 units of the lowest BIC value (ΔBIC $\leq$ 3) as competing models, and used the sum-of-weights (SW) probability of variable occurrence in competing models to identify the most robust predictors of soil δ^{15}N values (Galipaud and others 2014). For the BIC analysis of factors related to soil net N mineralization, we excluded percent nitrification as a predictor variable but included soil δ^{15}N to evaluate how well this stable isotope metric integrates soil N availability.

Our metric of fire history draws from an extensive dataset on fire history and stand development across our study area, based on sampling of 124 transects that resulted in determination of establishment dates for 3088 trees (Tepley and others 2013). This work identified 6 age-structure types that represent stand development trajectories driven by fires of varying frequency and severity across the landscape. We reduced these to two grouped classes based on data in Tepley and others (2013). The first group (FireGroup 1) includes age-structure types 1–3, which represent stands either lacking evidence of fire for more than 400 years (type 1) or stands that burned at relatively low severity where the fire did not generate large enough canopy openings to enable new establishment of Douglas-fir, a shade-intolerant species (types 2 and 3); we expect limited regeneration of shade-intolerant, N-fixing *Ceanothus* shrubs in these stand types. The second group (FireGroup 2) includes age-structure types 4–6, which all have evidence of at least one fire since the late eighteenth century that opened the canopy enough to enable new regeneration of shade-intolerant Douglas-fir. We expect high potential for regeneration of N-fixing *Ceanothus* shrubs in these stand types. This second group includes stands that burned at high severity and contain few if any trees more than 200 years old (type 5) and stands that burned at moderate severity and include Douglas-fir trees more than 200 years old at an average density of 24 and 45 trees ha^{-1} in types 4 and 6, respectively, above a younger post-fire cohort of Douglas-fir (Tepley and others 2013). Thus, our fire-history metric distinguishes stands that have had a substantial canopy-opening disturbance resulting from intense fire within the last about 200 years (FireGroup 2) from those that have either remained unburned or only experienced low-severity fire within the last 200 years that left the canopy largely intact (FireGroup 1).

We used SYSTAT 13 (Chicago, Illinois) for statistical analyses, with significance set at $P \leq 0.05$. Pearson correlation with Bonferroni corrected probabilities was used to evaluate collinearity in variables used in BIC analysis. The effect of fire history, a categorical variable, was evaluated as least squares means adjusted for the most common covariates in competing BIC models. Relationships among continuous site variables and soil δ^{15}N values were evaluated using least squares linear regression and non-linear (form $y = A/[x - B]$) regression. The homogeneity of slopes test was used to compare slopes of linear regressions. Classification and regression tree analysis was used to determine a breakpoint in the relationship of topographic slope to soil δ^{15}N.

RESULTS

In the paired comparison of 12 old-growth and 12 young (logged and burned) forests of contrasting fast and slow succession, we found that both stand age and successional rate contributed to significant differences in N cycle metrics, with no interactions (Table 2). We therefore focus on how either stand age (and associated disturbance) or successional rate influenced N and δ^{15}N patterns. Mineral soil (0–10 cm) δ^{15}N values were significantly lower in

Table 2. Mineral Soil (0–10 cm) and Foliar C, N, and δ^{15}N Values in Paired Young and Old-Growth Forests of Slow and Fast-Successional Rates

Forest type	Soil total C (mg kg^{-1})	Soil total N (mg kg^{-1})	Soil C:N	Soil δ^{15}N (‰)	Foliar N (%)	Foliar δ^{15}N (‰)	$\epsilon_{f\text{–}s}$ (‰)
Young stands							
Slow	10.62 ± 1.64	0.31 ± 0.07	36.2 ± 2.46	2.15 ± 0.33	1.14 ± 0.04	−2.82 ± 0.35	−4.98 ± 0.40
Fast	11.95 ± 2.14	0.35 ± 0.06	33.7 ± 1.04	3.29 ± 0.17	1.18 ± 0.02	−2.34 ± 0.49	−5.62 ± 0.50
Old-growth stands							
Slow	9.96 ± 1.22	0.29 ± 0.05	34.6 ± 3.30	3.15 ± 0.27	1.01 ± 0.02	−2.89 ± 0.35	−6.04 ± 0.34
Fast	10.62 ± 1.64	0.35 ± 0.09	30.3 ± 2.52	3.74 ± 0.34	1.04 ± 0.03	−2.56 ± 0.51	−6.30 ± 0.66
Significant effects	None	None	Rate, age	Rate, **age**	***Age***	None	***Age***

Significant treatment effects identified by split-plot ANOVA, with significance values of $P < 0.05$ in standard text, $P < 0.01$ in bold text, and $P < 0.001$ in bold italics.

young post-disturbance forests than in old-growth forests. Stands with slow succession displayed both lower mineral soil δ^{15}N values, and greater declines in soil δ^{15}N (1.0‰ decline, old-growth minus young forests) than fast-successional forests (0.45‰ decline). Foliar δ^{15}N values did not vary significantly with stand age or successional rate. Old-growth forests displayed a significantly wider δ^{15}N span between foliage and soil (that is, larger absolute $\epsilon_{f\text{–}s}$ values) and lower foliar N concentrations than did young post-disturbance forests (Figure 2), but these metrics did not differ with successional rate. Forest floor and mineral soil %C and %N did not differ by stand age or successional rate, but fast-successional sites had significantly lower mineral soil C:N than slow sites, as well as a non-significant trend towards lower forest floor C:N ($P = 0.10$, data in Appendix in Electronic Supplementary Material). Old-growth forests displayed lower mineral soil C:N, higher extractable soil C and lower extractable soil C:N than young post-disturbance forests. Neither extractable N nor net N mineralization differed systematically with stand age or successional rate.

Analysis of the larger suite of all 60 sites using BIC model selection identified seven competing models (ΔBIC $\leq$ 3) as potential predictors of landscape-level soil δ^{15}N variation (Table 3). The best model contained soil C:N, N mineralization, slope, age, and FireGroup (Table 3). None of these variables exhibited significant collinearity (Table 4). Of these variables, soil C:N, N mineralization, and slope occurred in all competing models (SW = 1.0), age occurred in six of the seven models (SW = 0.92), and FireGroup occurred in five of the seven models (SW = 0.60). For other variables appearing in competing models, MAT appeared in five models (SW = 0.59), forest floor N in two models (SW = 0.38), and forest floor C:N in one model (SW = 0.06), and all three variables exhibited significant collinearity (Table 4).

For net N mineralization, BIC model selection using all 60 sites identified three competing models (ΔBIC $\leq$ 3) as potential predictors (Table 3). The variables soil C, soil N, and soil δ^{15}N (all SW = 1.0) appeared in all competing models (Table 3). Soil C and N exhibited significant collinearity (Table 4), but neither correlated to soil δ^{15}N values. Slope (SW = 0.21) and forest floor N (SW = 0.16) each occurred in one of the competing models.

Individual analyses of significant predictor variables provide more detailed information on factors shaping soil δ^{15}N and N mineralization patterns. For the categorical variable FireGroup, we found after controlling for the most common BIC predictors (that is, soil C:N, net N mineralization, and slope) that soil δ^{15}N values across all 60 sites were significantly ($P = 0.02$) lower in sites where severe wildfire had opened the canopy in the prior 200 years (FireGroup 2, mean = 2.88‰, SE = 0.11‰, $n = 28$) than in forests with no or minor wildfire for over 400 years (FireGroup 1, mean = 3.25‰, SE = 0.11‰, $n = 32$, Figure 3). This effect was unchanged by considering only natural, unlogged stands ($n = 45$) (FireGroup 2: mean = 3.01‰, SE = 0.11‰, $n = 25$ vs. FireGroup 1: mean = 3.43‰, SE = 0.13‰, $n = 20$).

Bivariate plots of continuous variables yielded many significant relationships, though sometimes with low precision (low r^2), as expected from the large number of significant predictors in competing BIC models. The relationships among different N cycling metrics were fairly consistent. Net N mineralization increased with soil N ($r^2 = 0.52$, $P < 0.001$) and soil C (r^2 $0.25 = P < 0.001$) and was inversely related to soil C:N ($r^2 = 0.20$, $P < 0.001$). Net nitrification and extractable N also increased with soil N concentration and decreased with soil C:N (all $P \leq 0.05$, not shown). However, the relationships of various N cycling metrics to soil δ^{15}N values were less clear. Soil C:N was negatively related to soil δ^{15}N ($r^2 = 0.20$, $P = 0.0003$) (Figure 4), suggesting high-N availability (low C:N) was associated with high soil δ^{15}N values. Removal of 6 points with C:N greater than 40 weakened this relationship ($r^2 = 0.12$, $P = 0.01$), but did not significantly alter the slope ($P = 0.99$, homogeneity of slopes test). In contrast, patterns in both N mineralization and nitrification suggested low-N availability led to high soil δ^{15}N values ($r^2 = 0.06$–0.09, both $P < 0.03$), and soil N was unrelated to soil δ^{15}N ($P = 0.34$, not shown).

Forest succession measured as stand age resulted in a weak yet significant increase in soil δ^{15}N values ($r^2 = 0.14$, $P = 0.004$, $n = 60$; Figure 5). This relationship remained unchanged by removing young logged stands to consider only unlogged forests (slope = 0.0011 vs. 0.0012, respectively, $P = 0.91$, homogeneity of slopes test). It also remained unchanged by removing very old forests (ca. 650–800+ years, $n = 4$; slope = 0.0011 vs. 0.0017, $P = 0.41$, homogeneity of slopes test), although the regression improved slightly ($r^2 = 0.20$, $P < 0.001$, $n = 56$). Succession also drove a very weak decline in percent nitrification ($r^2 = 0.07$, $P = 0.03$), but no pattern in forest floor C:N ($P = 0.37$), soil C:N ($P = 0.56$) nor N mineralization ($P = 0.19$).

Soil δ^{15}N values declined as topographic slope increased ($r^2 = 0.20$, $P < 0.001$, $n = 60$, Figure 5). Classification and regression tree analysis identified a breakpoint in this relationship at 32.0% slope (=17.7°). Applying separate linear regressions to either side of this breakpoint revealed that soil δ^{15}N values varied significantly only on steeper topographic slopes ($y = -0.047x + 3.995$, $r^2 = 0.11$, $P = 0.04$, $n = 38$), but not gentler ones ($y = -0.005x + 3.554$, $r^2 = 0.001$, $P = 0.91$, $n = 22$). Considered on average, soil δ^{15}N values were significantly lower on steeper topographic slopes (average = 2.83‰, SE = 0.13‰, $n = 38$) than on gentler slopes (average = 3.49‰, SE = 0.16‰, $n = 22$) (t test, $P = 0.003$).

DISCUSSION

Soils are the largest N pool in temperate forests, with turnover times several orders of magnitude longer than N in vegetation, making soil δ^{15}N val-

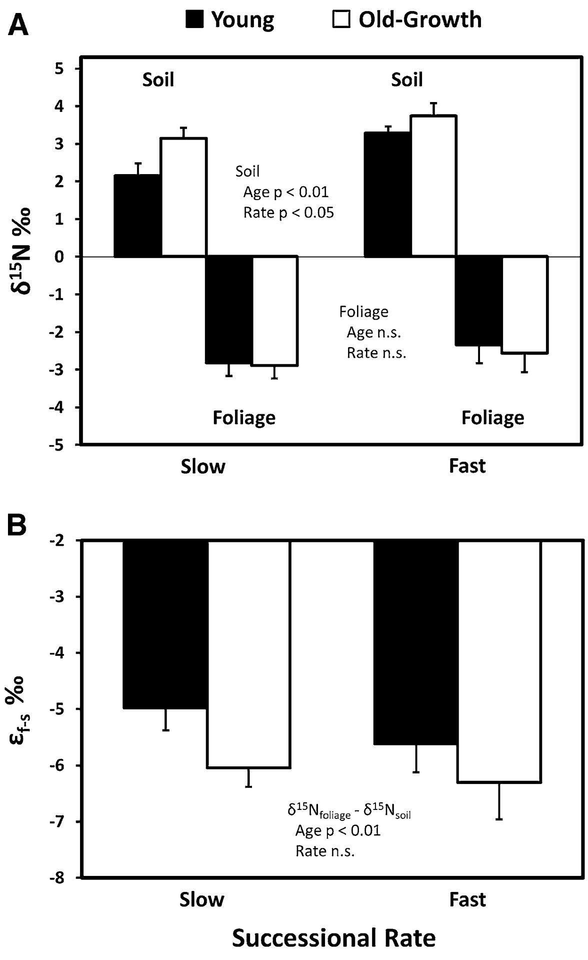

Figure 2. Successional rate and stand-age effects on (**A**) δ^{15}N values in mineral soil (0–10 cm) and foliage and (**B**) δ^{15}N span between foliage and mineral soil ($\epsilon_{\text{f–s}}$). Young stands are recovering from logging and broadcast burning, whereas old-growth stands are undisturbed. *Error bars* represent ± 1 SE. Significant effects are shown in figure panels.

ues useful for integrating long-term ecosystem N cycles. Disturbances are suggested to increase soil δ^{15}N values via a range of pathways that disrupt N cycling and promote N loss, including the removal of vegetation and surface organic horizons (Högberg 1997; Dunnette and others 2014), fractionation via biomass combustion (Huber and others 2013), and fractionation via nitrate loss and denitrification (Pardo and others 2002; Boeckx and others 2005). Surprisingly, we find an opposite pattern, where both forest logging and severe historic wildfire lowered soil δ^{15}N values for decades to centuries after disturbance. It is possible that sampling 40–50 years after logging and burning, and our wildfire record spanning 200–400 years, may have missed transient increases in soil δ^{15}N immediately after disturbance. Nevertheless, the overall decline in soil δ^{15}N values we observed

Table 3. Models Within ΔBIC ≤ 3 of the Best Model for Predicting Mineral Soil (0–10 cm) δ^{15}N Values (Top) and Net N Mineralization (Bottom) Across all 60 Sites

Model	BIC	ΔBIC
BIC model selection		
Soil δ^{15}N		
−SoilCN, −NMin, −Slope, Age, −FireGroup	118.942	0
−SoilCN, −NMin, −Slope, Age, −MAT, FFN	119.522	0.580
−SoilCN, −NMin, −Slope, Age	119.820	0.878
−SoilCN, −NMin, −Slope, Age, −FireGroup, −MAT	120.065	1.123
−SoilCN, −NMin, −Slope, Age, −FireGroup, −MAT, FFN	120.210	1.268
−SoilCN, −NMin, −Slope, −FireGroup, −MAT	121.211	2.269
−SoilCN, −NMin, −Slope, Age, −MAT, FFN, −FFCN	121.757	2.815
Net N mineralization		
SoilC, SoilN, −Soilδ^{15}N	412.555	0
SoilC, SoilN, −Soilδ^{15}N, Slope	414.760	2.205
SoilC, SoilN, −Soilδ^{15}N, FFN	415.365	2.810

See Methods for detailed explanation of the variables used in the analyses. All models shown outperformed the null models for soil δ^{15}N (BIC = 157.560) and for net N mineralization (BIC = 412.555). The direction of relationships is shown for negative correlations, with no sign for positive correlations.

Table 4. Pearson Correlation Coefficients for Predictor Variables Used in BIC Model Selection for Mineral Soil (0–10 cm) δ^{15}N Values and Net N Mineralization Across All 60 Sites

	AGE	MAT	MAP	CMD	Slope	Aspect	Heat load	Fire Group	FFC	FFN	FFCN	SoilC	SoilN	SoilCN	Soilδ^{15}N	Nmin
MAT	−0.29															
MAP	0.40	−***0.83***														
CMD	−0.33	***0.90***	−***0.92***													
Slope	0.08	0.23	−0.14	0.21												
Aspect	−0.03	0.23	−0.25	0.21	−0.08											
Heat load	0.03	0.05	−0.12	0.04	−*0.45*	***0.62***										
FireGroup	−0.14	−0.04	−0.16	−0.05	−0.22	0.00	0.14									
FFC	0.33	−***0.56***	*0.47*	−***0.57***	−0.20	−0.05	0.03	0.14								
FFN	0.20	−***0.64***	***0.56***	−***0.62***	−0.31	−0.02	0.10	0.26	***0.76***							
FFCN	−0.12	***0.53***	−***0.49***	***0.51***	0.38	−0.01	−0.15	−0.28	−**0.52**	−***0.92***						
SoilC	−0.09	−0.28	0.25	−0.16	0.12	−0.12	−0.29	−0.19	−0.11	0.10	−0.15					
SoilN	−0.05	−0.24	0.18	−0.08	0.06	−0.10	−0.21	−0.10	−0.11	0.22	−0.31	***0.88***				
SoilCN	−0.08	−0.10	0.16	−0.18	0.22	−0.14	−0.29	−0.13	0.08	−0.25	0.37	0.09	−0.34			
Soilδ^{15}N	0.37	−0.22	0.19	−0.19	−0.44	0.02	0.28	−0.12	0.15	0.19	−0.26	−0.28	−0.13	−*0.45*		
Nmin	−0.17	0.01	−0.07	0.11	0.05	−0.09	−0.13	0.10	−0.19	0.09	−0.17	**0.51**	***0.72***	−0.39	−0.28	
%NO_3^-	−0.27	0.21	−0.22	0.20	0.06	0.11	−0.04	0.10	−0.24	−0.04	0.02	0.23	0.39	−0.25	−0.30	***0.57***

Bonferroni corrected significance as: $P < 0.05$ in italics, $P < 0.01$ in bold text, and $P < 0.001$ in bold italics.

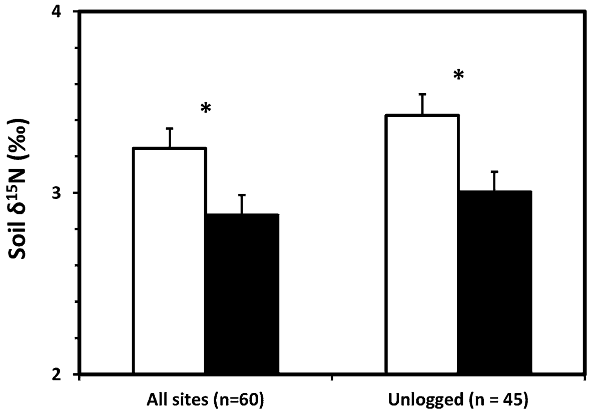

Figure 3. Influence of historic wildfire severity on mineral soil δ^{15}N values (0–10 cm) for all study sites (*left side*) and only unlogged sites (*right side*). *Open bars* indicate sites with no or minor wildfire for more than 400 years (FireGroup 1), *closed bars* indicate sites where severe wildfire opened the forest canopy at least once in the past 200 years (FireGroup 2). Values are least-squared means, error bars are ± 1 SE, and *asterisks* indicate significance at $P < 0.05$.

suggests that fractionating N losses have not dominated soil N fluxes throughout the period of forest recovery.

Relative Importance of Losses and Inputs: Fire, N Fixation, Leaching, and Denitrification

The decline in soil δ^{15}N values that we observed after disturbance is consistent with tight N cycling and retention in these unpolluted conifer forests (Sollins and others 1980; Vanderbilt and others 2003). Tree growth in these Douglas-fir forests is demonstrably N-limited (Peterson and Hazard 1990) and high soil C and C:N ratios foster rapid microbial N uptake (Hart and others 1994). These processes minimize fractionating N loss via nitrate leaching and denitrification to only very low levels, even after severe disturbance (Sollins and McCorison 1981; Vermes and Myrold 1992). Thus, other factors may shape declines in soil δ^{15}N values after disturbance. However, vegetation regrowth and N redistribution from soil to aboveground biomass typically increases mineral soil δ^{15}N values as forests recover from disturbance (Compton and others 2007), and we similarly found that foliage had lower δ^{15}N values than soil, with no difference in foliar δ^{15}N between young and old-growth forest. To explain post-disturbance declines in soil δ^{15}N, we therefore evaluate below two mechanisms whereby disturbance could add N at low δ^{15}N values to soil: (1) N transfer from disturbed vegetation to soil, and (2) post-disturbance N inputs from symbiotic N fixation.

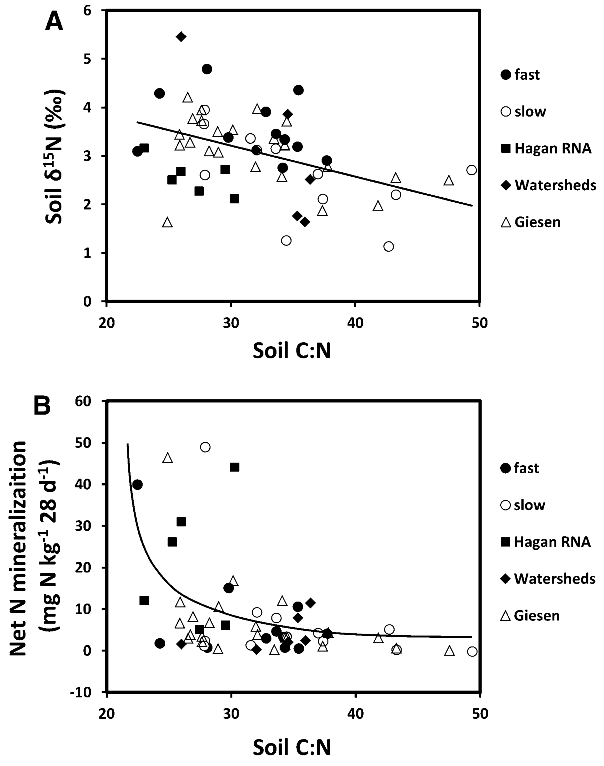

Figure 4. Mineral soil (0–10 cm) C:N versus (**A**) soil δ^{15}N values and (**B**) N mineralization. *Regression lines* include all points; *symbols* distinguish groups of study sites for the 60 plots (see Table 1). Linear regression line for (**A**) $y = -0.0649x + 5.1273$, $r^2 = 0.20$, $P < 0.001$ and non-linear regression for (**B**) $y = 73.6/(x - 20.0)$, $r^2 = 0.20$, $P < 0.001$.

Wildfire and logging in old-growth forests of the Pacific Northwest deposit considerable detritus, ash, and char on the soil surface, and can mix organic horizons into mineral soil, all of which may lower mineral soil δ^{15}N values. Using our soil and foliar δ^{15}N data from paired stands (Table 2), we calculate that conservative mixing of logging debris N from old-growth foliage (145 kg N ha^{-1}) into surface soil (1000 kg N ha^{-1}, 0–10 cm; Sollins and others 1980) would lower average surface soil δ^{15}N values from 3.5 to 2.7‰, which is similar to values measured in young logged forests (average = 2.72‰). Burning of logging debris could increase detrital δ^{15}N values up to 3‰ by combustion fractionation (Turekian and others 1998; Grogan and others 2000; Boeckx and others 2005; Saito and others 2007; Huber and others 2013), but accounting for this effect before mixing still yields a decline in soil δ^{15}N to 2.9‰. In contrast to our findings, studies of logging without subsequent

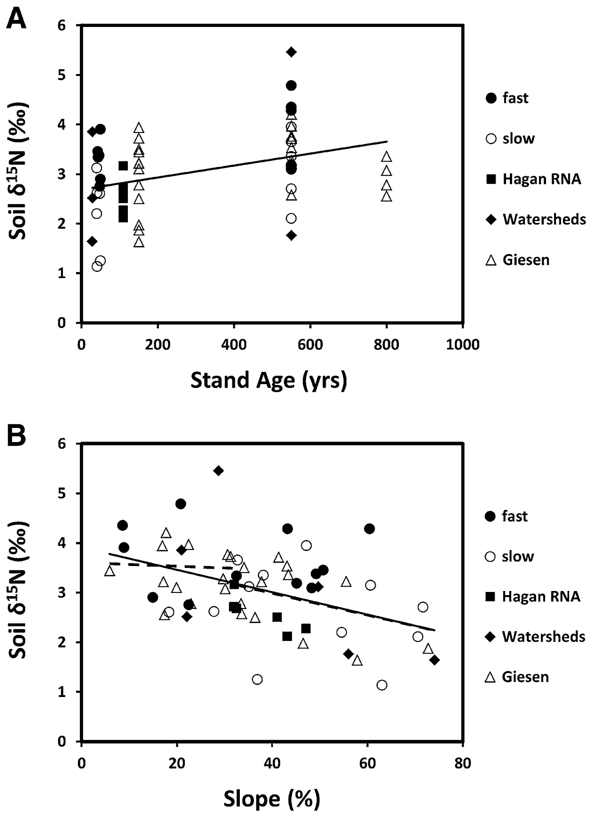

Figure 5. Relationships depicting (**A**) stand age versus soil δ^{15}N values and (**B**) slope versus soil δ^{15}N values. *Solid regression lines* include all points; *symbols* distinguish groups of study sites for the 60 plots (see Table 1). *Solid linear regression line* for (**A**) $y = 0.0012x + 2.691$, $r^2 = 0.14$, $P = 0.004$ and (**B**) $y = -0.0226x + 3.9157$, $r^2 = 0.20$, $P < 0.001$. *Dashed regression lines* in (**B**) separated by a breakpoint at 32% slope (~ 18°) identified by classification and regression tree analysis, with a significant relationship with soil δ^{15}N values only for steep slopes ($r^2 = 0.12$, $P = 0.03$, $n = 38$), but not gentler slopes ($r^2 = 0.0001$, $P = 0.96$, $n = 22$).

burning report slight increases or no change in soil δ^{15}N values (Pardo and others 2002; Sah and others 2006). It is possible that burning at our sites helped incorporate logging debris N into the fine earth fraction of mineral soil to lower soil δ^{15}N values, but other differences in fractionating N loss and recovery after disturbance among studies make this difficult to evaluate.

Biological N fixation is the second and more tractable mechanism that could lower soil δ^{15}N values at our sites after disturbance. The symbiotic N-fixing shrub snowbrush ceanothus (*Ceanothus velutinus* Douglas ex Hook.) frequently dominates early succession in these forests (Halpern and Lutz 2013; Brown and others 2013) and sustains N fixation of 20–100 kg N ha^{-1} y^{-1} for several decades before succession to conifers (Binkley and others 1982; McNabb and Cromack 1983). Fixed N can lower soil δ^{15}N towards atmospheric values (Barrett and others 2002 Boutton and Liao 2010) and decomposition of *Ceanothus* biomass can add additional N to soil (Zavitovski and Newton 1968, Spears and others 2001). *Ceanothus* dominance and N fixation are especially favored in open sites with slow succession (Yelenik and others 2013), and this can explain the larger decline in soil δ^{15}N values we observed in slow-successional than fast-successional sites. Stable isotope mixing calculations using 0–10 cm mineral soil δ^{15}N values from paired old-growth and young-logged forests suggest plausible cumulative N fixation inputs (at 0‰) that are roughly twice as large in slow-successional sites (410 kg N ha^{-1}) than fast-successional sites (165 kg N ha^{-1}). This difference is consistent with a twofold longer period of shrub dominance supporting N-fixing *Ceanothus* in slow-successional sites (Nesje 1996). These estimates do not account for potential redistribution of N to deeper soil, to other plants, or to losses. Notably, symbiotic N fixers were not important in contrasting studies where soil δ^{15}N increased or remained constant after logging (Pardo and others 2002; Sah and others 2006). The coherence of our stable isotope calculations with observed patterns of *Ceanothus* dominance and N fixation through succession makes symbiotic N fixation a highly plausible explanation for declining soil δ^{15}N values after logging disturbance.

Long-Term Changes in N Biogeochemistry

Our chronosequence revealed that severe wildfire leaves a legacy of lower soil δ^{15}N values that persists for centuries after disturbance, extending our findings from young logged forests to older stands. For both the entire set of 60 forests we studied, and a reduced set of 45 unlogged forests, we found that severe wildfire in the prior 200 years resulted in an approximately 0.4% decline in surface soil δ^{15}N values. This legacy of historic wildfire (Figure 3) was smaller than the decline recorded after clearcut logging and burning (~1.2‰ decline, Figure 2), which may reflect lower N fixation in natural forest gaps than clearcuts, or different effects of wildfire versus logging on ash, char, and detritus inputs. This difference can be only partially explained by time since disturbance, because soil δ^{15}N values increased only very slowly over centuries of succession (0.001‰ y^{-1}, or 0.1‰/100 years, Figure 5). Mineral soil N availability (Table 3) and N pool size (Giesen and others 2008) did not display a wildfire legacy, however, suggesting that post-disturbance N inputs replaced possible soil losses to burning and plant N uptake. The subtle yet significant signal of historic wildfire that we detected on soil δ^{15}N values provides additional evidence of tight N cycling in these forests, and connects wildfire effects on stand-structure and succession (Tepley and others 2013) to soil N biogeochemistry.

Bioclimatic controls on the distribution and activity of symbiotic N fixers appear to broadly shape soil δ^{15}N values and N fertility across Pacific Northwest forests. Both this study from the Oregon Cascades and our prior work from Oregon Coast Range found a negative relationship between mean annual temperature and soil δ^{15}N (Table 3, and Perakis and others 2011). This is consistent with warmer temperatures stimulating the nitrogenase enzyme and N fixation (Houlton and others 2008), causing soil δ^{15}N to approach the value of atmospheric inputs. This pattern contrasts with the global positive relationship between temperature and soil δ^{15}N that is thought to reflect faster N cycling and fractionating loss at warmer temperatures (Amundson and others 2003), and raises the possibility that N fixation is relatively more important for N balances of Pacific Northwest forests than elsewhere. Even within Oregon forests, the importance of N fixation varies considerably depending on location and the species of symbiotic N fixer present. In the Cascades forests we studied, N fixation by dense stands of early-successional *Ceanothus* shrubs roughly replaces the quantity of N lost in wildfire, but not enough N is added to overcome N-limitation (for example, Binkley and others 1982; McNabb and Cromack 1983). In contrast, the early-successional N-fixing tree *Alnus rubra* dominates in the more maritime Coast Range forests, and can fix much more N than is lost in fire, ultimately promoting long-term N accumulation and natural N saturation (Perakis and Sinkhorn 2011; Perakis and others 2011, 2012, 2013). Even though both forests occupy the broadly distributed western hemlock vegetation zone, their stark contrast in N fertility illustrates the key role that N fixation plays in the biogeochemistry of climate-wildfire interactions.

We observed small net changes in foliar and soil N isotopes and N availability during 800+ years of succession from young to old-growth forest. Foliar δ^{15}N values often decline throughout secondary succession (Compton and others 2007; Wang and others 2007; Hyodo and others 2013), which suggests declining N availability (Craine and others 2009; Perakis and others 2011), and we did observe lower foliar N (Table 2) but no trend in foliar δ^{15}N with stand age ($r^2 = 0.002$). For soils, δ^{15}N values often track N availability and loss through succession, with values close to inputs in primary succession when N losses are low (Hobbie and others 1998; Menge and others 2011; Pérez and others 2014a, b) and increasing with greater N availability and loss throughout soil development (Brenner and others 2001; Vitousek 2004). However, soil N availability measured in laboratory incubations did not vary in clear fashion over 800 years of succession in our study, nor in our comparisons of paired young and old-growth forest, suggesting N availability does not explain the small increase we observed in soil δ^{15}N values throughout succession. This increase more likely reflects the redistribution of N with low δ^{15}N values from soil to aboveground biomass (Billings and Richter 2006; Compton and others 2007). However, we observed a much lower rate of soil δ^{15}N increase over secondary succession (0.001‰ y^{-1}) compared to N-polluted forests recovering from agricultural abandonment (~0.01‰ y^{-1}, Compton and others 2007), reinforcing the idea that low-N availability constrains soil δ^{15}N dynamics in our forests.

Wildfire is an infrequent yet dominant disturbance in many Pacific Northwest forests (Whitlock 1992). Thus, our finding of lower soil δ^{15}N values after disturbance may not capture whole-ecosystem δ^{15}N patterns over complete disturbance and recovery cycles. Wildfire combustion can dominate long-term N losses from forests (Johnson and others 2004; Giesen and others 2008; Bormann and others 2008) and lead to oscillation in soil and ecosystem δ^{15}N values as N is gained and lost through time (Perakis and others 2011). Soil δ^{15}N values varied widely across our fire-dominated landscape, yet despite low nitrate leaching and denitrification, our average surface soil δ^{15}N values (3.1‰) were higher than temperate forests globally (~2.5‰, Martinelli and others 1999). We infer that wildfire, by driving combustion losses of vegetation and detritus with relatively low δ^{15}N values, contributes to higher ecosystem δ^{15}N values at steady-state. We show in Table 5 our best estimates of leaching, gaseous, and wildfire N loss for forests at HJ Andrews over a 500 year wildfire disturbance cycle, and associated average ecosystem δ^{15}N values at steady-state. Fire combustion of vegetation and detritus dominates (~75%) long-term N loss in our calculation, and leads to elevated ecosystem δ^{15}N values. We note that these average δ^{15}N values do not capture potential changes within cycles of fire N loss and post-disturbance recovery. Full accounting of how N in deep soil and vegetation pools changes after disturbance (for example,

Table 5. Steady-State δ^{15}N Calculations Evaluating the Relative Influence of Fractionating N Loss by Leaching, Gas, and Wildfire over 500-Year Fire Cycle at HJ Andrews

	δ^{15}N or ϵ (‰)[1]	500 year flux (kg N ha^{-1})[2]	% of N loss
Inputs (δ^{15}N)	−1		
Losses (ϵ)			
Leaching (inorganic N)	−0.8	58	4.4
Leaching (organic N)	0	250	18.9
Gaseous	−16	16	1.2
Fire	−5.7	1000	75.5
Weighted average	−4.5		
Ecosystem δ^{15}N (inputs − losses)	3.5		
Ecosystem without leaching	4.9		
Ecosystem without gas loss	3.4		
Ecosystem without fire	−0.1		

---

[1] δ^{15}N values of N inputs, and isotope effects (ϵ) for N leaching and gas loss, from Houlton and Bai (2009). Isotope effect for fire combustion is foliage depletion relative to soil (−5.7‰, Table 2), assuming forest floor δ^{15}N values similar to foliage (Perakis and others 2011), and conservatively assuming no additional gaseous fractionation during heating and combustion. Weighted average of N loss considers cumulative losses of all pathways over 500 years. Ecosystem δ^{15}N at steady-state is estimated as δ^{15}N (inputs) − ϵ (weighted average) after Fry (2006).

[2] 500 year cumulative N leaching based on long-term watershed fluxes at HJ Andrews (Vanderbilt and others 2003). Gaseous N loss based on soil N_2O fluxes in disturbed (0.05 kg N ha^{-1} y^{-1} for 50 y) and mature (0.001 kg N ha^{-1} y^{-1} for 450 y) forests at HJ Andrews, scaled to include additional loss via N_2 (3.5x) and NO_x (1x) based on Houlton and Bai (2009). Fire N loss from Giesen and others (2008).

Compton and others 2007) would better inform successional patterns of δ^{15}N oscillation in fire-dominated systems, and reconcile our observed post-disturbance declines in surface soil δ^{15}N values with their expected increase at steady-state. Whereas denitrification and nitrate leaching are most likely to increase soil δ^{15}N values in high-N ecosystems (Högberg 1997), we expect that fire increases steady-state ecosystem δ^{15}N values most strongly in low-N ecosystems, where fire dominates N budgets (Johnson and others 2004) and where biomass has both lower δ^{15}N values and is a larger proportion of total ecosystem N (Perakis and others 2011).

Role of Topography

We found that soil δ^{15}N values were more enriched on gentle than steep slopes, as observed previously in both cultivated and pastured soils (Karamanos and Rennie 1980), in tropical montane forest soils (Hilton and others 2013), and in global data syntheses (Amundson and others 2003). Higher soil δ^{15}N values on gentler slopes can reflect more denitrification fractionation due to greater soil moisture (Sutherland and others 1993) or a longer residence time of soils permitting full expression of fractionating losses (Amundson and others 2003). However, we did not find a correlation between soil δ^{15}N values and nitrification, even though nitrification correlates with denitrification enzyme activity in these forests (Griffiths and others 1998). Aspect and elevation, but not slope, correlate with denitrification enzymes at HJ Andrews (Griffiths and others 2009), and overall denitrification rates are exceedingly low (Vermes and Myrold 1992), suggesting that denitrification does not control slope effects on soil δ^{15}N values at our sites.

Our data are consistent with the idea that steeper topographic slopes promote non-fractionating erosional losses of soil organic matter and decrease the residence time of soil N, causing soil δ^{15}N values to approach the signature of inputs on steep slopes (Amundson and others 2003; Hilton and others 2013). Steep slopes in our study region accelerate soil erosion (Roering and others 1999) and decrease soil C pools (Homann and others 1995), and should cause similar changes in soil N (Table 4). Although concentrations of 0–10 cm mineral soil C and N did not correlate with slope, we did not determine rock content and bulk density, nor deep soil C and N, which are needed to calculate pools (Homann and others 1995). Our surface soil δ^{15}N data nevertheless appeared to capture slope effects that were similar to other landscapes. Using classification and regression tree analysis, we identified a significant break in the relationship between slope and soil δ^{15}N values at 32% (~18°), with the relationship remaining significant only for steeper slopes (dotted lines, Figure 5). This 18° breakpoint is similar to a 20° breakpoint suggested previously as a topographic control on soil δ^{15}N values in montane forests (Hilton and others 2013). Soil turnover times in our steep montane landscape are likely on the order of 10^4 years, longer than the 10^1–10^3 year frequency of wildfire disturbance (Poage and others 2009; Tepley and others 2013). Thus, wildfire effects on soil δ^{15}N values appear to operate within longer-term constraints set by topography. Wildfire disturbance may also interact with steep topography to accelerate erosional loss, decrease soil residence times, and promote early-successional species (including N fixers), all of which may drive soil δ^{15}N values towards atmospheric inputs.

Summary

Overall, our results highlight the importance of disturbance-related processes in shaping soil δ^{15}N values over long-term succession in N-poor, unpolluted temperate forests. Standard conceptual models based on studies of more N-rich and/or polluted forests typically infer that fractionating N losses by soil biological N processing, and their stimulation by disturbance, lead to increases in soil δ^{15}N values. As a counterpoint to this biotic-loss view of ecosystem δ^{15}N development, we find that abiotic pathways of N loss such as fire combustion and soil erosion can also shape soil N and δ^{15}N patterns over ecosystem succession. Our results suggest that N lost in severe disturbance can be replenished in the short-term by high rates of symbiotic N fixation, resulting in transient declines in soil δ^{15}N values with no appreciable long-term change in soil N availability. Over long-term soil development, steady-state calculations suggest that recurring wildfire can increase ecosystem δ^{15}N via combustion loss of biomass and detritus with relatively low δ^{15}N values. Both short- and long-term wildfire effects on δ^{15}N values are likely to be most pronounced in N-limited ecosystems with low losses of available N. Expression of these disturbance effects will also vary with their recurrence interval (decadal to century for most forest wildfires) relative to the turnover time of soil N (millennial). This interplay of biotic and abiotic factors as controls on long-term ecosystem N balances is exemplified in fire-prone montane forests, especially where symbiotic N fixers form an important component of early-successional vegetation.

ACKNOWLEDGMENTS

We thank Mark Harmon, Kari O’Connell, Tom Giesen, Mark Schulze, and Patti Haggerty for site information, Chris Catricala, Morgan Luce, Bill Rugh, and Aaron Thiel for field and laboratory assistance, and Helga Van Miegroet and two anonymous reviewers for comments on the manuscript. Any use of trade names is for descriptive purposes only and does not imply endorsement by the US Government. This research was funded by National Science Foundation grant DEB 021-8088 to the Long-Term Ecological Research Program at the HJ Andrews Experimental Forest.

REFERENCES

Amundson R, Austin AT, Schuur EAG, Yoo K, Matzek V, Kendall C, Uebersax A, Brenner D, Baisden WT. 2003. Global patterns of the isotopic composition of soil and plant nitrogen. Glob Biogeochem Cycles 17:31-1–-10.

Aranibar JN, Macko SA, Anderson IC, Potgieter A, Sowry R, Shugart HH. 2003. Nutrient cycling responses to fire frequency in the Kruger National Park (South Africa) indicated by stable isotopes. Isot Environ Healt Stud 39:141–58.

Bai E, Houlton BZ, Wang YP. 2012. Global nitrogen hotspots across terrestrial ecosystems. Biogeosciences 9:3287–304.

Bai E, Boutton TW, Liu F, Wu XB, Archer SR. 2013. ^{15}N isoscapes in a subtropical savanna parkland: spatial-temporal perspectives. Ecosphere 4:art4.

Barrett JE, Johnson DW, Burke IC. 2002. Abiotic nitrogen uptake in semiarid grassland soils of U.S. Great Plains. Soil Sci Soc Am J 66:979–87.

Bierlmaier FA, McKee A. 1989. Climatic summaries and documentation for the primary meteorological station. In: Andrews HJ, Ed. Experimental forest, 1972 to 1984. Portland: USDA Forest Service, GTR- PNW-242.

Billings S, Richter DD. 2006. Changes in stable isotopic signatures of nitrogen and carbon during 40 years of forest development. Oecologia 148:325–33.

Binkley D, Cromack K, Fredriksen RL. 1982. Nitrogen accretion and availability in some snowbrush ecosystems. For Sci 28:720–4.

Boeckx B, Paulino L, Oyarzun C, van Cleemput O, Godoy R. 2005. Soil δ^{15}N patterns in old-growth forests of southern Chile as integrator for N-cycling. Isot Environ Health Stud 41:249–59.

Bormann BT, Homann PS, Darbyshire RL, Morrissette BA. 2008. Intense forest wildfire sharply reduces soil C and N: the first direct evidence. Can J For Res 38:2771–83.

Boutton TW, Liao JD. 2010. Changes in soil nitrogen storage and δ^{15}N with woody plant encroachment in a subtropical savanna parkland landscape. J Geohys Res 115:G03019.

Bowman DM, Balch JK, Artaxo P, Bond WJ, Carlson JM, Cochrane MA, D’Antonio CM, Defries RS, Doyle JC, Harrison SP, Johnston FH, Keeley JE, Krawchuk MA, Kull CA, Marston JB, Moritz MA, Prentice IC, Roos CI, Scott AC, Swetnam TW, van der Werf GR, Pyne SJ. 2009. Fire in the Earth system. Science 5926:481–4.

Brenner DL, Amundson R, Baisden WT, Kendall C, Harden J. 2001. Soil N and ^{15}N variation with time in a California annual grassland ecosystem. Geochem Cosmoch Acta 65:4171–86.

Brown MJ, Kertis J, Huff MH. 2013. Natural tree regeneration and coarse woody debris dynamics after a forest fire in the western Cascade Range. Portland: USDA Forest Service, PNW-RP-592.

Compton JE, Hooker TD, Perakis SS. 2007. Ecosystem N distribution and δ^{15}N during a century of forest regrowth after agricultural abandonment. Ecosystems 10:1197–208.

Craine JM, Elmore AJ, Aidar MPM, Bustamante M, Dawson TE, Hobbie EA, Kahmen A, Mack MC, McLauchlan KK, Michelsen A, Nardoto GB, Pardo LH, Peñuelas J, Reich PB, Schuur EAG, Stock WD, Templer PH, Virginia RA, Welker JM, Wright IJ. 2009. Global patterns of foliar nitrogen isotopes and their relationships with climate, mycorrhizal fungi, foliar nutrient concentrations, and nitrogen availability. New Phytol 183:980–92.

Dunnette PV, Higuera PE, McLauchlan KK, Derr KM, Briles CE, Keefe MH. 2014. Biogeochemical impacts of wildfires over four millennia in a Rocky Mountain subalpine watershed. New Phytol 203:900–12.

Fry B. 2006. Stable isotope ecology. New York: Springer.

Galipaud M, Gillingham MAF, David M, Dechaume-Moncharmont F-X. 2014. Ecologists overestimate the importance of predictor variables in model averaging: a plea for cautious interpretations. Methods Ecol Evol 5:983–91.

Giesen TW, Perakis SS, Cromack K Jr. 2008. Four centuries of soil carbon and nitrogen change after stand-replacing fire in a forest landscape in the western Cascade Range of Oregon. Can J For Res 38:2455–64.

Giglia SK. 2004. Spatial and temporal patterns of ''super-old'' Douglas-fir trees of the central western Cascades, Oregon. MS Thesis, Oregon State University.

Griffiths RP, Homann PS, Riley R. 1998. Denitrification enzyme activity of Douglas-fir and red alder forest soils of the Pacific Northwest. Soil Biol Biochem 30:1147–57.

Griffiths RP, Madritch MD, Swanson AK. 2009. The effects of topography on forest soil characteristics in the Oregon Cascade Mountains. For Ecol Manag 257:1–7.

Grogan P, Bruns TD, Chapin FS. 2000. Fire effects on ecosystem nitrogen cycling in a Californian bishop pine forest. Oecologia 122:537–44.

Halpern CB, Lutz JA. 2013. Canopy closure exerts weak controls on understory dynamics: a 30-year study of overstory-understory interactions. Ecol Monogr 83:221–37.

Hart SC, Nason GE, Myrold DD, Perry DA. 1994. Dynamics of gross nitrogen transformations in an old growth forest: the carbon connection. Ecology 75:880–91.

Hilton R, Galy A, West AJ, Hovius N, Roberts GG. 2013. Geomorphic control on the δ^{15}N of mountain forests. Biogeosciences 10:1693–705.

Hobbie EA, Macko SA, Shugart HH. 1998. Patterns in N dynamics and N isotopes during primary succession in Glacier Bay, Alaska. Chem. Geol. 152:3–11.

Högberg P. 1997. ^{15}N natural abundance in soil-plant systems. New Phytol 137:179–203.

Homann P, Sollins P, Chappell H, Stangenberger A. 1995. Soil organic carbon in a mountainous, forested region: relation to site characteristics. Soil Sci Soc Am J 59:1468–75.

Houlton BZ, Bai E. 2009. Imprint of denitrifying bacteria on the global terrestrial biosphere. Proc Natl Acad Sci 106:21713–16.

Houlton BZ, Wang YP, Vitousek PM, Field CB. 2008. A unifying framework for dinitrogen fixation in the terrestrial biosphere. Nature 454:327–31.

Huber E, Bell T, Adams M. 2013. Combustion influences on natural abundance nitrogen isotope ratio in soil and plants following a wildfire in a sub-alpine ecosystem. Oecologia 173:1063–74.

Hyodo F, Kusaka S, Wardle DA, Nilsson MC. 2013. Changes in stable nitrogen and carbon isotope ratios of plants and soil across a boreal forest fire chronosequence. Plant Soil 364:315–23.

Johnson DW, Susfalk RB, Caldwell TG, Murphy JD, Miller WW, Walker RF. 2004. Fire effects on carbon and nitrogen budgets in forests. Water Air Soil Pollut Focus 4:263–75.

Karamanos RE, Rennie DA. 1980. Changes in natural ^{15}N abundance associated with pedogenic processes in soil. II. Changes on different slope positions. Can J Soil Sci 60:365–72.

Klopsch MW. 1985. Structure of mature Douglas-fir stands in a western Oregon watershed and implications for interpretation of disturbance history and succession. MS Thesis, Oregon State University.

Kranabetter JM, Saunders S, MacKinnon JA, Klassen H, Spittlehouse DL. 2013. An assessment of contemporary and historic nitrogen availability in contrasting coastal Douglas-Fir forests through δ^{15}N of tree rings. Ecosystems 16:111–22.

Martinelli LA, Piccolo MC, Townsend AR, Vitousek PM, Cuevas E, McDowell WH, Robertson GP, Santos OC, Treseder K. 1999. Nitrogen stable isotopic composition of leaves and soil: tropical versus temperate forests. Biogeochemistry 46:45–65.

McCune B. 2007. Improved estimates of incident radiation and heat load using non-parametric regression against topographic variables. J Veg Sci 18:751–4.

McLauchlan KK, Craine JM. 2012. Species-specific trajectories of nitrogen isotopes in Indiana hardwood forests, USA. Biogeosciences 9:867–74.

McLauchlan K, Higuera PE, Gavin DG, Perakis SS, Mack MC, Alexander H, Battles J, Biondi F, Buma B, Colombaroli D, Enders S, Engstrom DR, Hu FS, Marlon RR, Marshall J, McGlone M, Nave LE, Shuman BN, Smithwick E, Urrego D, Wardle DA, Williams CJ, Williams JJ. 2014. Reconstructing disturbances and their biogeochemical consequences over multiple timescales. Bioscience 64:105–16.

McNabb DH, Cromack K Jr. 1983. Dinitrogen fixation by a mature *Ceanothus velutinus* (Dougl.) stand in the western Oregon Cascades. Can J Microbiol 29:1014–21.

Menge DNL, DeNoyer JL, Lichstein JW. 2010. Phylogenetic constraints do not explain the rarity of nitrogen-fixing trees in late-successional temperate forests. PLoS ONE 5:e12056.

Menge DNL, Baisden WT, Richardson SJ, Peltzer DA, Barbour MM. 2011. Declining foliar and litter δ^{15}N diverge from soil, epiphyte, and input δ^{15}N along a 120,000 year temperate rainforest chronosequence. New Phytol 190:941–52.

Murtaugh PA. 2009. Performance of several variable-selection methods applied to real ecological data. Ecol Lett 12:1061–8.

Nesje AM. 1996. Spatial patterns of early forest succession following harvest in Lookout Creek Basin, OR. Master's Thesis, Oregon State University, Corvallis, OR.

Pardo LH, Hemond HF, Montoya JP, Fahey TJ, Siccama TG. 2002. Response of natural abundance of ^{15}N in forest soils to high nitrate loss following clear-cutting. Can J For Res 32:1126–36.

Perakis SS, Kellogg CH. 2007. Imprint of oaks on nitrogen availability and δ^{15}N in California grassland-savanna: a case of enhanced N inputs? Plant Ecol 191:209–20.

Perakis SS, Sinkhorn ER. 2011. Biogeochemistry of a temperate forest nitrogen gradient. Ecology 92:1481–91.

Perakis SS, Sinkhorn ER, Compton JE. 2011. δ^{15}N constraints on long-term nitrogen balances in temperate forests. Oecologia 167:793–807.

Perakis SS, Matkins JJ, Hibbs DE, Huso MM. 2012. N_2-fixing red alder indirectly accelerates ecosystem nitrogen cycling. Ecosystems 15:1182–93.

Perakis SS, Sinkhorn ER, Catricala CE, Bullen TD, Fitzpatrick J, Hynicka JD, Cromack K Jr. 2013. Forest calcium depletion and biotic retention along a soil nitrogen gradient. Ecol Appl 23:1947–61.

Pérez CA, Thomas FM, Silva WA, Segura B, Gallardo B, Armesto JJ. 2014a. Patterns of biological nitrogen fixation during 60,000 years of forest development on volcanic soils from south-central Chile. N Z J Ecol 38:189–200.

Pérez CA, Aravena JC, Silva WA, Enríquez JM, Fariña JM, Armesto JJ. 2014b. Ecosystem development in short-term postglacial chronosequences: N and P limitation in glacier forelands from Santa Inés Island, Magellan Strait. Austral Ecol 39:288–303.

Peterson CE, Hazard JW. 1990. Regional variation in growth response of coastal Douglas-fir to nitrogen fertilizer in the Pacific Northwest. For Sci 36:625–40.

Poage NJ, Weisberg PJ, Impara PC, Tappeiner JC, Sensenig TS. 2009. Influences of climate, fire, and topography on contemporary age structure patterns of Douglas-fir at 205 old forest sites in western Oregon. Can J For Res 39:1518–30.

Rastetter EB, Vitousek PM, Field C, Shaver GR, Herbert D, Ågren GI. 2001. Resource optimization and symbiotic N fixation. Ecosystems 4:369–88.

Roering JJ, Kirchner JW, Dietrich WE. 1999. Evidence for nonlinear, diffusive sediment transport on hillslopes and implications for landscape morphology. Water Resour Res 35:853–70.

Sah SP, Rita H, Ilvesniemi H. 2006. ^{15}N natural abundance of foliage and soil across boreal forests of Finland. Biogeochemistry 80:277–88.

Saito L, Miller WW, Johnson DW, Qualls RG, Provencher L, Carroll E, Szameitat P. 2007. Fire effects on stable isotopes in a Sierran forested watershed. J Environ Qual 36:91–100.

Schroeder TA, Cohen WB, Zhiqiang Y. 2007. Patterns of forest regrowth following clearcutting in Western Oregon as determined from Landsat time-series. For Ecol Manag 243:259–73.

Scott EE, Perakis SS, Hibbs DE. 2008. δ^{15}N patterns of Douglas-fir and red alder riparian forests in the Oregon Coast Range. For Sci 54:140–7.

Shearer G, Kohl DH. 1989. Estimates of N_2 fixation in ecosystems: the need for and basis of the ^{15}N natural abundance method. In: Rundel PW et al., Eds. Stable isotopes in ecological research. Berlin: Springer. p 342–74.

Smithwick EAH, Turner MG, Mack MC, Chapin FS. 2005. Postfire soil N cycling in northern conifer forests affected by severe, stand-replacing wildfires. Ecosystems 8:163–81.

Sollins P, McCorison FM. 1981. Nitrogen and carbon solution chemistry of an old-growth coniferous forest watershed before and after cutting. Water Resour Res 17:1409–18.

Sollins P, Grier CC, McCorison FM, Cromack K Jr, Fogel R, Fredriksen RL. 1980. The internal element cycles of an old-growth Douglas-fir ecosystem in western Oregon. Ecol Monogr 50:261–85.

Spears JDH, Lajtha K, Caldwell BA, Pennington SB, Vanderbilt K. 2001. Species effects of *Ceanothus velutinus* versus *Pseudotsuga menziesii*, Douglas-fir, on soil phosphorus and nitrogen properties in the Oregon Cascades. For Ecol Manag 149:205–16.

Stephenson N. 1998. Actual evapotranspiration and deficit: biologically meaningful correlates of vegetation distribution across spatial scales. J Biogeogr 25:855–70.

Stock WD, Wienand KT, Baker AC. 1995. Impacts of invading N_2-fixing Acacia species on patterns of nutrient cycling in two Cape ecosystems: evidence from soil incubation studies and ^{15}N natural abundance values. Oecologia 101:375–82.

Sutherland RA, vanKessel C, Farrell RE, Pennock DJ. 1993. Landscape-scale variations in plant and soil nitrogen-15 natural abundance. Soil Sci Soc Am J 57:169–78.

Tepley AJ, Swanson FJ, Spies TA. 2013. Fire-mediated pathways of stand development in Douglas-Fir/Western Hemlock forests of the Pacific Northwest, USA. Ecology 94:1729–43.

Tepley AJ, Swanson FJ, Spies TA. 2014. Post-fire tree establishment and early cohort development in conifer forests of the western Cascades of Oregon, USA. Ecosphere 5:80.

Turekian VC, Macko S, Ballentine D, Swap R, Garstang M. 1998. Causes of bulk carbon and nitrogen isotopic fractionations in the products of vegetation burn. Chem Geol 152:181–92.

Vanderbilt KL, Lajtha K, Swanson F. 2003. Biogeochemistry of unpolluted forested watersheds in the Oregon Cascades: temporal patterns of precipitation and stream nitrogen fluxes. Biogeochemistry 62:87–117.

Vermes J-F, Myrold DD. 1992. Denitrification in forest soils of Oregon. Can J Forest Res 22:504–12.

Vitousek PM. 2004. Nutrient cycling and limitation: Hawai'i as a model system. Princeton: Princeton University Press.

Vitousek PM, Reiners WA. 1975. Ecosystem succession and nutrient retention: a hypothesis. Bioscience 25:376–81.

Vitousek PM, Mooney HA, Lubchenco J, Melillo JM. 1997. Human domination of Earth's ecosystems. Science 277:494–9.

Wang LP, Shaner JL, Macko S. 2007. Foliar δ^{15}N patterns along successional gradients at plant community and species levels. Geophys Res Lett 34:L16403.

Wang T, Hamann A, Spittlehouse DL, Murdock TQ. 2012. ClimateWNA—high-resolution spatial climate data for western North America. J Appl Meteorol Clim 51:16–29.

Weisberg PJ, Swanson FJ. 2003. Regional synchroneity in fire regimes of western Oregon and Washington, USA. For Ecol Manag 172:17–28.

Whitlock C. 1992. Vegetational and climatic history of the Pacific Northwest during the last 20,000 years. Northwest Environ J 8:5–28.

Yelenik SG, Perakis SS, Hibbs DE. 2013. Regional constraints to biological nitrogen fixation in post-fire forest communities. Ecology 94:739–50.

Zavitovski J, Newton M. 1968. Ecological importance of snowbrush *Ceanothus velutinus* in the Oregon Cascades. Ecology 49:1113–45.